

Stochastic Fermi Acceleration of sub-Relativistic Electrons and Its Role in Impulsive Solar Flares

Robert Selkowitz and Eric G. Blackman

Dept. of Physics and Astronomy, and Laboratory for Laser Energetics, University of Rochester, Rochester NY, 14627

ABSTRACT

We reexamine stochastic Fermi acceleration (STFA) in the low energy (Newtonian) regime in the context of solar flares. The particle energization rate depends on a dispersive term and a coherent gain term. The energy dependence of pitch angle scattering is important for determining the electron energy spectrum. For scattering by whistler wave turbulence, STFA produces a quasi-thermal spectrum. A second well-constrained scattering mechanism is needed for STFA to match the observed 10 – 100keV non-thermal spectrum. We suggest that STFA most plausibly acts as phase one of a two phase particle acceleration engine in impulsive flares: STFA can match the thermal spectrum below 10keV, and possibly the power law spectrum between 10 and 100keV, given the proper pitch angle scattering. However, a second phase, such as shock acceleration at loop tops, is likely required to match the spectrum above the observed knee at 100keV. Understanding this knee, if it survives further observations, is tricky.

Subject headings: acceleration of particles, Sun: flares, Sun: X-Rays, gamma-rays

1. Introduction

Fermi acceleration was first proposed as a mechanism for cosmic ray acceleration (Fermi 1949, 1954). In the original model, compressive perturbations in the Galactic magnetic field, associated with molecular clouds, reflect charged particles. If these clouds converge, the particles gain energy over time. If they diverge, the particles lose energy. Later, it was realized (Bell 1978; Axford, Leer, & Skadron 1978; Krymskii 1977; Blandford & Eichler 1987), that shock fronts are another site of Fermi Acceleration. In the shock acceleration model, charged particles stream into magnetic perturbations in the post-shock region, reflect, and are scattered back across the shock by pre-shock Alfvén waves. Repeated reflections

steadily accelerate particles to a power law distribution. This has been studied extensively (e.g. Jones & Ellison 1991). If the shock thickness is determined by the ion gyroradius then ions are picked up out of the thermal population but electrons must be injected at energies at or above the thermal energy by a factor of the ratio of proton to electron mass, (m_p/m_e), to incur power law acceleration. The injection process is a critical outstanding problem for many applications of shock acceleration. Shock Fermi acceleration is commonly referred to as first order Fermi Acceleration because the sign of the energy gain after each cycle is positive and $dE/dt \propto v_c/v$, where E and v are the electron energy and speed, and v_c the velocity of the magnetic compression.

Fermi acceleration can also take place in a fully turbulent plasma. There, the mirroring sites are turbulent perturbations, typically fast mode magnetohydrodynamic waves, randomly distributed throughout the plasma (e.g. Achterberg (1984)). Electrons encounter these perturbations such that there is a stochastic distribution of energy gaining and energy losing reflections. As is demonstrated below, there is a net dissipation of turbulent energy into high energy electrons. Because the energy gaining and energy losing reflections are equal to first order, STFA is often referred to as second order Fermi acceleration and proceeds more slowly than the first order process. For STFA, $dE/dt \propto (v_c/v)^2$.

STFA has been considered extensively as the acceleration mechanism in impulsive solar flares, (e.g. LaRosa et al. (1996)). Observations of these flares show hard X-ray emission with a downward breaking power law spectrum extending from 10keV to at least 0.5MeV with the break energy narrowly distributed around $E_{br} = 100\text{keV}$ and a thermal distribution at energies below 10keV (Dulk et.al. 1992; Krucker, & Lin 2002). The time structure of the emission shows distinct spikes of duration 1s and typical energy 10^{26}erg (Aschwanden, et.al. 1995). Non-thermal emission occurs principally at the footpoints of the soft X-ray loop, and to a lesser extent at a loop-top hard X-ray source (Tsuneta 1996; Masuda, et.al. 1996). Brown (1971) has shown that the emission at a dense target is consistent with Bremsstrahlung radiation by electrons accelerated to a power law energy distribution at some height above the target; in impulsive flares the acceleration site can be associated with the loop-top region, while the thick target is associated with the footpoints. We demonstrate that STFA is possibly responsible for the acceleration of electrons below 10keV, while first order Fermi processes at the loop-top fast shock may produce the highest energy electrons. In this picture STFA also provides power law distributed electrons in the range $10\text{keV} < E < 100\text{keV}$, thus satisfying the shock injection criterion and producing the observed spectral break at 100keV. It is shown that in order to produce this spectrum the pitch angle scattering must obey the restriction that the scattering distance, λ_P , is inversely proportional to the energy of the scattered electron in the 10 – 100keV range. Matching the knee is difficult, requiring either a cutoff in the secondary pitch scattering at 100keV, or the sudden onset of yet another

pitch scattering agent with a much shorter wavelength. While both are possible, these requirements provide a serious challenge to STFA models of electron acceleration.

It is important to note that the downward break is not observed in all impulsive solar flares. Indeed, Dulk et.al. (1992) observed a spread in break energies and spectral indexes. Some of their flares exhibited no discernible break, or even some upward breaks (ankles). In this paper we address the fundamental process of STFA, and show how it can accommodate the downward breaking spectra observed in a subset of impulsive flares. The general form of the electron spectra we model is illustrated in figure 1. We assume a thick target Bremsstrahlung emission model where the electron spectral index δ and the photon spectral index γ are related by $\delta = \gamma + 1$ (Brown 1971; Tandberg-Hanssen & Emslie 1988). The data shown are mean values taken from the flares studied by Dulk et.al. (1992): $E_{br} = 100\text{keV}$, $\delta = 4$ below E_{br} , and $\delta = 5.25$ above E_{br} .

Furthermore, not all flares are observed to be dominated by electron acceleration. A recent flare observed by Hurford et.al. (2003) clearly shows regions of emission which are dominated by X-ray emission from electrons as well as regions which are dominated by gyrosynchrotron emission from MeV/nucleon ions. Proton and ion emission appears to be associated primarily associated with larger flare loops. Miller and Roberts (1995); Miller, Emslie, and Brown (2004) propose that this can be explained by a two stage process for ion acceleration. First, ions are accelerated via gyroresonance to speeds of roughly v_A by Alfvén waves, and subsequently are accelerated preferentially over electrons by magnetosonic waves. They argue convincingly for the gyroresonant acceleration by Alfvén waves on the basis of relative ion abundances. However, it is unclear that the second stage acceleration by magnetosonic modes must be resonant. It appears that the second stage is consistent with STFA. In any event, proton acceleration in long flare loops presents an interesting problem for acceleration models, in that super-Alfvénic protons must be preferentially accelerated over electrons, but electron acceleration still must be dominant in shorter loops. In this work, we presume that the loops are sufficiently short that protons remain sub-Alfvénic. Longer loops, and the effects of proton acceleration on the shaping of the observed Bremsstrahlung X-ray spectra from high energy electrons, require further study.

STFA is found to depend on two competing effects which we refer to as the steady and diffusive acceleration rates. The steady rate represents the net acceleration of electrons due to the slight advantage of head-on or energy gaining reflections over catch-up or energy losing reflections. The diffusive term represents the spreading of the electron distribution function as a result of the stochastic nature of the reflections. Longair (1994) treats the two effects together using the Fokker-Planck equation. Likewise, Park and Petrosian (1995) discuss general solutions of a simplified Fokker-Planck equation for STFA. In a follow-up

work, Park, Petrosian, and Schwartz (1997) apply their solution to solar flares. While they produce spectra consistent with observations, they do not discuss the physics of electron escape. Furthermore, they focus mainly on the regime above 100keV. Some past treatments of STFA in impulsive flares focused exclusively on the diffusive term. LaRosa et al. (1996) derives the diffusive acceleration rate using simple physical arguments. Chandran (2003) derives the diffusive term using both phenomenological arguments and quasi-linear theory. The latter also includes Coloumb losses as a small correction; this is of note since the Coloumb loss term is mathematically similar to a negative steady acceleration term. Herein we derive the steady term and compare it to the diffusive term, finding the steady acceleration to be dominant in the non-relativistic regime for impulsive flares. As will be seen, our steady term differs slightly from that of some previous calculations such as that in Longair (1994) in its dependence on the turbulent magnetic fluctuation strength. This arises because we average only over the pitch angle phase space for which STFA operates in magnetic mirroring, whereas Longair (1994) averaged over all pitch angles in considering a more generic form of Fermi acceleration. A similar averaging over all pitch angles is performed in Skilling (1975); Webb (1983).

We first review the basic Fermi process using a test particle approach. We then derive an expression for the mean acceleration of electrons in a turbulent plasma via STFA, and compare this to the diffusive STFA derived by LaRosa et al. (1996). Finally, we discuss the trapping of electrons in the turbulent accelerating region and show that at non-relativistic energies, the electron spectrum depends strongly on the energy dependence of pitch angle scattering. For scattering by whistler wave turbulence, the emerging spectrum is quasi-thermal. In order to produce the 10 – 100keV power law in solar flares, we show that there must be an additional source of pitch angle scattering which has a length scale inversely dependent on electron energy; this mechanism is tightly constrained. The existence of such a pitch angle scattering mechanism is yet to be determined. This brings to the fore the most pressing difficulty with STFA models of electron acceleration; the pitch angle scattering requirements are stringent and might not be possible to meet.

2. The Fermi Acceleration Process

Consider a particle of charge q traveling with gyroradius r_G in a magnetic field of strength B (Fermi 1949, 1954; Spitzer 1956). The charge follows a helical path, orbiting the field line while also moving parallel (or anti-parallel) to the field line. Taking the condition for circular motion and the Lorentz force

$$F = qv_{\perp}B = \frac{mv_{\perp}^2}{r_G}, \quad (1)$$

where q is the electron charge, and applying conservation laws for angular momentum and kinetic energy ($r_G v_{\perp}$ and v^2 constant) yields

$$\frac{qL}{mE} = \frac{\sin^2 \theta}{B}, \quad (2)$$

where L is the angular momentum of the charge, E the kinetic energy, and $v \sin \theta = v_{\perp}$ relates the total velocity to the component perpendicular to the field line. The pitch angle, θ , is the angle between the field line and the velocity vector. As the charge enters a region of increasing B , such as a magnetic compression, the pitch angle evolves according to

$$\frac{\sin^2 \theta_1}{B + \delta B} = \frac{\sin^2 \theta}{B} \quad (3)$$

where δB is the increase in field strength and θ_1 is the pitch angle at field strength $B + \delta B$. When $\sin \theta_1 = 1$, the charge cannot penetrate further into the compression, and reflects. This process, known as magnetic mirroring, is commonly used to confine laboratory plasmas (Dendy 1990). It follows immediately that mirroring will not occur at a given compression unless the initial pitch angle satisfies

$$\sin^2 \theta \geq \frac{B}{B + \delta B}. \quad (4)$$

Fermi (1949, 1954) showed that moving magnetic mirrors, in particular molecular clouds, can accelerate charges. In the cloud's frame of reference (primed), mirroring results in only a change in the sign of v'_{\parallel} , the component of the initial velocity of the charge parallel to the field line in the compression's rest frame. Let us work for the moment in the limit where the compression speed and the particle speed are both $\ll c$. Transforming to the lab frame, $\delta v_{\parallel} = \pm 2v_c$, where v_c is the drift velocity of the cloud. The positive (negative) sign is for head-on (catch-up) reflections between the charge and cloud. Catch-up reflections are defined as those where the components of the compression and charge velocities parallel to the field line have the same sign. Head on reflections are those where the parallel components have opposite signs. The net change in energy from a reflection is given by

$$\delta E_{\pm} = \frac{m}{2}(v_f^2 - v_0^2) = \frac{m}{2}(2\delta v_{\parallel}v_0 \cos(\theta) + (\delta v_{\parallel})^2) = (2m)(\pm v_c v_{\parallel} + v_c^2), \quad (5)$$

where v_f and v_0 are the speeds after and before reflection, m is the mass of the charge, and $v_{\parallel} = v_0 \cos(\theta)$. Head-on reflections result in a positive energy change, while catch-up

reflections can result in a negative energy change when $v_{\parallel} > v_c$. In both types of reflection, there is the positive term proportional to v_c^2 .

One can repeat this derivation using Lorentz transformations in place of the Galilean transformations to generalize this result to particles of any energy scattered by compressions which are still restricted to non-relativistic velocities. For a derivation see Longair (1994); we simply cite the result:

$$\delta E_{\pm R} = 2E \left[\pm \frac{v_c v_{\parallel}}{c^2} + \frac{v_c^2}{c^2} \right], \quad (6)$$

where c is the speed of light in vacuum. Over time, charges trapped between converging magnetic compressions are subject to only head-on reflections, and are accelerated to higher energies.

Notice that the change in momentum of a Fermi accelerated electron is solely in the component parallel to the mean field. This corresponds to an increase in the electron's pitch angle. As an extreme example, consider an electron of initial energy E_0 with pitch angle in the mean field B approaching $\pi/2$. Upon doubling the electron's energy via Fermi acceleration, the pitch angle in the mean field is reduced to $\pi/4$. Clearly, acceleration to high energy must be accompanied by some additional scattering agent which isotropizes electron pitch angles on a short time scale, otherwise Fermi acceleration shuts off after small accelerations as pitch angles evolve out of the range given by (4). The well known problem of pitch angle scattering remains largely unsolved (e.g. Achterberg (1981); Melrose (1974); LaRosa et al. (1996)).

Fermi acceleration is distinct from the transit time damping (TTD) treated, for example, in Miller, Larosa, & Moore (1996). TTD is the magnetic analog of Landau Damping. In TTD, electrons (or ions) which are near gyroresonance with waves of wavenumber k are pushed towards the resonance by field gradients in the wave which alter the parallel component of the velocity. Gradients in the electron velocity spectrum result in a net damping or enhancement of the waves. In the presence of a spectrum of waves, an electron can drift from resonance at k to $k \pm \delta k$ and so forth, eventually reaching high energies. Fermi Acceleration, however, is a non-resonant interaction. Electrons will mirror at a compression regardless of energy provided that the pitch angle is sufficiently large. TTD is often referred to as resonant Fermi Acceleration because the two processes rely on similar physics. Table 1 lists the relevant length and time scales for STFA in impulsive flares.

Length scale	Description	Time scale	Description
L_T	Turbulent outer scale	τ_S	Steady STFA acceleration time
λ_T	Turbulent eddy scale	τ_D	Diffusive STFA acceleration time
λ_{\parallel}	Parallel eddy scale	τ_{ED}	Turbulent eddy time
λ_{\perp}	Perpendicular eddy scale	τ_p	Pitch angle scattering time
λ_{SF}	Effective STFA scale		
λ_p	MFP for pitch angle scattering		
λ_{wh}	λ_p for scattering by whistlers		
λ_C	Constrained λ_p for 10 – 100keV		

Table 1: Table of length and time scales relevant to STFA in impulsive flares.

3. Stochastic Fermi Acceleration

We now consider the behavior of charges in a turbulent magnetic plasma where magnetosonic modes provide the sites of magnetic mirroring. This scenario differs from first order Fermi acceleration by shocks in two ways. 1) Consecutive mirroring events are not coherent, but rather stochastically distributed between head-on and catch-up. 2) The turbulent cascade governs the acceleration efficiency; the system picks out a scale where acceleration competes with the cascade. In the solar corona plasma, v_c , the velocity of the magnetic compressions, is the phase speed of the magnetosonic modes, which is roughly the Alfvén speed for the fast mode and the sound speed (c_s) for the slow mode. Typically, thermal electrons in the corona are super-Alfvénic and non-relativistic, $v_A \ll v_0 \ll c$, and $\beta \sim 0.05$; we will solve the STFA problem in this regime.

3.1. Determination of the Steady Acceleration Rate

Recall that the energy gain from a typical reflection is given in Eq.(5) to be $\delta E_{\pm} = 2m(\pm v_{\parallel} v_c + v_c^2)$. We define three parameters: R , the total rate of reflections; R_+ , the rate of head-on reflections; and R_- , the rate of catch-up reflections. The relation $R = R_+ + R_-$ is automatically satisfied by this definition as all reflections must be of either the head-on or catch-up type. This allows us to write the approximate acceleration rate as the sum of a coherent term and an incoherent term:

$$\left(\frac{dE}{dt}\right)_S = 2m[(R_+ - R_-)v_{\parallel}v_c + (R_+ + R_-)v_c^2], \quad (7)$$

where the subscript S is used to distinguish our derived acceleration rate from that of LaRosa et al. (1996). The first term, proportional to $(R_+ - R_-)$ represents the mean acceleration due to the offset in the rates of the two types of reflection. The second term, proportional to $(R_+ + R_-) = R$, the total reflection rate, represents the coherent term. This expression gives a full description of the mean acceleration of charges by the non-relativistic STFA process. To evaluate it in a particular plasma requires the determination of the head-on and catch-up reflection rates R_+ and R_- .

In order to obtain R_+ and R_- , consider the path a charge takes to encounter a mirror. Note that there is a distinction between an encounter and a mirroring because of the pitch angle condition for reflection. We take the fraction of encounters which reflect to be F and assume that this fraction is the same for both head-on and catch-up encounters: $F = F_+ = F_-$. This assumption is often taken in the regime where $v \gg v_c$ (LaRosa et al. 1996). While this assumption is not strictly true, the effects of relaxing it are negligible. In Appendix B we repeat this calculation without assuming $F_+ = F_-$. There is a well defined mean distance between encounters, λ_T as well as a relative velocity between the particle and the compression $v_{\pm} = v_{\parallel} \pm v_c$. The small difference in the head-on and catch-up speeds is responsible for the offset in rates. For each type of encounter, the mean separation is $2\lambda_T$ and the rate of reflections of any sort is specified by the general relation $R = Fv_{rel}\lambda$, with v_{rel} the relative velocity between the particle and compression, yielding

$$\begin{aligned} R_+ &= F \frac{v_{\parallel} + v_c}{2\lambda_T} \\ R_- &= F \frac{v_{\parallel} - v_c}{2\lambda_T} \\ R &= R_+ + R_- = F \frac{v_{\parallel}}{\lambda_T}. \end{aligned} \tag{8}$$

The offset in rates is thus

$$R_+ - R_- = F \frac{v_c}{\lambda_T}, \tag{9}$$

and we can rewrite the average acceleration rate as

$$\left(\frac{dE}{dt} \right)_S = 2mF \frac{v_{\parallel} v_c^2}{\lambda_T} + 2mF \frac{v_{\parallel} v_c^2}{\lambda_T} = 4mF \frac{v_{\parallel} v_c^2}{\lambda_T}, \tag{10}$$

with the associated acceleration time scale $\tau_S = E / \left(\frac{dE}{dt} \right)_S$. We thus see that the acceleration due to the offset in head-on and catch-up reflection rates and the acceleration from the coherent term in v_c are equal.

To simplify the derivation of the electron spectrum, we recast (10) as

$$\left(\frac{dE}{dt}\right)_S = 4mv_c^2 R = \frac{dE}{dM} \frac{dM}{dt}, \quad (11)$$

where we used (8) and define M as the total number of reflections experienced by an electron, $dM/dt = R$, and

$$dE/dM = 4mv_c^2. \quad (12)$$

The quantity dE/dM , the mean acceleration of an electron per reflection, will be of particular use when examining electron escape in section 4.

3.2. Comparison to the Diffusive Acceleration Rate

A different approach was taken by LaRosa et al. (1996). They set $R_+ = R_-$ in the $v \gg v_c$ regime and studied the diffusion of particles through energy space via random walk. The starting point in their calculation of the electron acceleration was the timescale for the e-folding of a charged particle's energy in the turbulent plasma

$$\frac{1}{\tau_D} = \frac{1}{E} \left(\frac{dE}{dt}\right)_D = \frac{F}{N\delta t}, \quad (13)$$

where N is the number of mirrorings required to double the particle's energy and δt is the time between encounters. They set $R_+ - R_- = 0$, and also dropped the last term in v_c^2 in Eq 6. From (7) and (10) it is clear that if one of their two assumptions is valid the other must also apply, and $(dE/dt)_S = 0$ in that limit. Under these assumptions δE_+ and δE_- are equal in magnitude, and from the standard solution of an evenly weighted random walk $N = (E/\delta E)^2$. The acceleration rate is then

$$\left(\frac{dE}{dt}\right)_D = \frac{E}{\tau_D} = F \frac{\delta E^2}{E} \frac{v_{\parallel}}{\lambda_T} = \frac{8F}{\lambda_T} \frac{mv_c^2 v_{\parallel}^3}{v_0^2}, \quad (14)$$

where v_0 is the total initial speed and the subscript D is used to denote LaRosa et al's diffusive acceleration rate.

To complete the calculation of the acceleration rates, we must obtain F and average over pitch angles. The minimum accessible pitch angle for reflection is related to F by

$$F = \cos(\theta_{min}) = \left(\frac{\delta B}{B}\right)^{1/2}, \quad (15)$$

where we have applied the reflection condition from (4). In the regime where the compression ratio $\delta B/B \ll 1$, which will apply to the plasma of interest, and taking the assumption that pitch angles are isotropic gives $\langle \cos(\theta) \rangle = \cos(\theta_{min})/2$ and $\langle \cos^3(\theta) \rangle = \cos^3(\theta_{min})/4$. We now write the averaged acceleration rates as

$$\left(\frac{dE}{dt}\right)_S = 4mF \frac{\langle v_{\parallel} \rangle v_c^2}{\lambda_T} = \frac{2m}{\lambda_T} (v_c^2 v) \left(\frac{\delta B}{B}\right), \quad (16)$$

$$\left(\frac{dE}{dt}\right)_D = \frac{8F}{\lambda_T} \frac{m v_c^2 \langle v_{\parallel}^3 \rangle}{v_0^2} = \frac{2m}{\lambda_T} (v_c^2 v) \left(\frac{\delta B}{B}\right)^2. \quad (17)$$

What do these two acceleration rates represent? $(dE/dt)_S$ is the steady growth of the mean kinetic energy due to the drain of turbulence by the combined effects the slightly non-zero $(R_+ - R_-)$ and the coherent v_A^2 term: a shift of the mean electron energy to higher energy. On the other hand, $(dE/dt)_D$ represents the diffusion of energies away from the mean via random walk: a spreading of the distribution. The relative importance of the two is fixed by their ratio

$$\zeta = \frac{\left(\frac{dE}{dt}\right)_S}{\left(\frac{dE}{dt}\right)_D} = \frac{B}{\delta B} \quad (18)$$

The combined result of the action of both processes on an initially narrow Gaussian energy distribution is shown in Fig.2 where we have chosen $\zeta = 65$. and assume that electrons do not escape. Thus we can examine the evolution of electron energy spectra solely due to the influence of the two acceleration rates. As ζ is increased, the steady (mean growth) term becomes increasingly dominant over the diffusive (distribution widening) term. To understand STFA in a particular plasma, both acceleration rates must be calculated. In the event that the diffusive rate is very small compared to the steady growth rate, it can be ignored. The steady growth rate is always faster than the diffusive growth rate for $a > 1$. As will be shown later, $\zeta \sim 100$ in flare plasmas, and the diffusive term is negligible.

It is very important to note that our result differs from the standard for Fermi Acceleration, in which both the diffusive and steady terms depend on the same power of $\delta B/B$. This difference arises as a result of the averaging over pitch angles. To correctly obtain $\langle \Delta E \rangle$, one must only average over those encounters which result in a reflection. For traditional STFA, the range of pitch angles which reflect is ultimately determined by the turbulent magnetic field strength. One factor of $\cos(\theta)$ in the expression to be averaged results in one factor of $(\delta B/B)^{1/2}$ in the acceleration rate. In other treatments, such as that of Longair

(1994); Webb (1983); Skilling (1975), the acceleration mechanism is assumed to act at all pitch angles. In this case, the averaging over $\cos(\theta)$ while maintaining the assumption of pitch angle isotropy, yields a numerical value with no δB dependence. In this regime, the diffusive and steady acceleration terms have the same relative strength at all levels of turbulence.

3.3. Specification of the Turbulent Cascade

This leaves $\delta B/B$ as the remaining parameter to be determined. It is related to the turbulent length scale λ_T through the cascade law. Magnetohydrodynamic (MHD) turbulence proceeds by the shredding of like sized eddies and subsequent formation of smaller eddies; energy input into eddies on a large (outer) length scale, L_T , cascades rapidly to smaller length scales on the eddy turnover time, τ_{ed} , and finally dissipates at λ_r , the dissipation scale. If the cascade obeys Komolgorov’s steady state assumption then the energy flow through all length scales is constant, and independent of the scale. This results in an inertial range between the scales L_T and λ_r where the turbulent energy density has a power law dependence on eddy size. The draining of turbulence at eddy size λ_r is usually determined by a micro-physical process, such as resistivity. When STFA is active, the turbulence can instead be drained by pumping energy into electrons. This sets another condition for STFA to proceed in a plasma: there must be some λ_{SF} which is greater than the resistive length scale at which the STFA timescale is shorter than the cascade time, otherwise the turbulence will drain at the resistive scale before STFA can produce an appreciable electron acceleration.

There are three major MHD wavemodes: Alfvén waves, and the fast and slow magnetosonic waves. Alfvén waves are purely transverse, and thus do not compress the magnetic field; they cannot participate in STFA. Both the fast and slow modes are compressive, and are in principle capable of Fermi acceleration. It has been argued that in low β plasmas such as the solar corona, the slow mode is rapidly dissipated via Landau damping (Achterberg 1981). However, more recent studies of MHD turbulence indicate that the cascade time for GS turbulence is significantly shorter than the electron damping time, and slow mode damping by electrons can be ignored in turbulent flare plasmas (Lithwick and Goldreich 2001). A key difference in the two analyses is that Lithwick and Goldreich (2001) treats MHD turbulence as inherently anisotropic, whereas Achterberg (1981) assumes isotropy. Furthermore, Maron (private communication) has shown in simulations which neglect damping that the slow mode may be driven with much higher total energy content than the fast mode at low β . A definitive resolution of the issue is beyond the scope of this paper. However, we should point out that up to this point, the calculation is independent of the choice of wave mode. There is one significant difference between the two, however: slow modes propagate

at roughly the sound speed ($v_c \sim c_s$) while fast modes propagate at roughly the Alfvén speed ($v_c \sim v_A$). It will be shown that due to the influence of pitch angle scattering, STFA is likely dominated by the fast mode.

MHD turbulence is in general anisotropic; the direction of any large scale mean magnetic field defines a preferred axis. Also, even if the turbulence is isotropic on large scales, smaller scales may see the larger scale turbulent structures as an effective mean field. Goldreich and Sridhar (1997) (hereafter, GS) modified the the Komolgorov assumption for the cascade of slow and Alfvén modes of MHD turbulence under the condition that the turbulence is anisotropic with scale λ_{\parallel} along the field line and λ_{\perp} perpendicular to the field line. The two directions are found to obey different cascade laws, with λ_{\parallel} cascading more weakly than λ_{\perp} . The parallel direction is of more importance to STFA, as it represents the distance along the field line between reflection sites. The GS power law for the parallel scale is (Goldreich and Sridhar 1997; Lithwick and Goldreich 2001)

$$\frac{\delta B}{B} = \left(\frac{\lambda_T}{L_T} \right)^{1/2}, \quad (19)$$

where B is the mean magnetic field strength, and δB is the turbulent field strength at parallel length scale λ_T .

The exact power law of MHD turbulence remains the subject of some debate, so for now we assume a general power law of form

$$\frac{\delta B}{B} = \left(\frac{\lambda_T}{L_T} \right)^{1/a}, \quad (20)$$

where $a > 1$ is an arbitrary index. Using the turbulent power spectrum and substituting for F from (15) we can rewrite the acceleration rates as

$$\begin{aligned} \left(\frac{dE}{dt} \right)_S &= \frac{2m}{\lambda_T} v_A^2 v \left(\frac{\lambda_T}{L_T} \right)^{1/a} = \frac{2}{L} m v_A^2 v \left(\frac{\lambda_T}{L_T} \right)^{(1/a)-1} \\ &\text{so that } \tau_S = \frac{1}{4} \frac{v L_T}{v_A^2} \left(\frac{\lambda_T}{L_T} \right)^{1-(1/a)} \\ \left(\frac{dE}{dt} \right)_D &= \frac{2m}{\lambda_T} v_A^2 v \left(\frac{\lambda_T}{L_T} \right)^{2/a} = \frac{m}{L} v_A^2 v \left(\frac{\lambda_T}{L_T} \right)^{(2/a)-1} \\ &\text{so that } \tau_D = \frac{1}{4} \frac{v L_T}{v_A^2} \left(\frac{\lambda_T}{L_T} \right)^{1-(2/a)}. \end{aligned} \quad (21)$$

For a typical turbulent cascade, where $\lambda_T < L_T$ and $a > 0$, $\tau_S < \tau_D$.

3.4. λ_{SF} and the Role of Pitch Angle Scattering

There remains the final step of determining the particular dissipation scale λ_{SF} at which the energy drain takes place. In order for STFA to overcome the cascade of MHD turbulence, it must drain energy at a rate equal to the input rate at the outer scale. If turbulent compressions are shredded and cascade faster than electrons can draw out energy via reflections, then the cascade continues to smaller length scales. At smaller scales, STFA is more rapid. STFA becomes competitive with the cascade at a scale determined by $(dE/dt)_S = dE_T/dt$. $(dE/dt)_S$ is acceleration rate of electrons and dE_T/dt is the cascade rate of turbulent energy, $nm_p v_A^3/L_T$. The STFA scale λ_{SF} is different for acceleration by the two compressive MHD modes.

For slow mode turbulence, $v_c = c_s$, and the balance is

$$\frac{2nm_e}{L_T} c_s^2 v \left(\frac{\lambda_T}{L_T} \right)^{(1/a)-1} = \frac{nm_p}{L_T} v_A^3. \quad (22)$$

Solving for λ_T/L_T and associating this particular λ_T with λ_{SF} gives

$$\frac{\lambda_{SF}}{L_T} = \left[\frac{1}{2} \frac{m_p}{m_e} \frac{v_A^3}{c_s^2 v} \right]^{\frac{a}{1-a}}. \quad (23)$$

In solar flares and a GS turbulent cascade ($a = 2$), $v_0 = 1.2 \times 10^9$ cm/s, $c_s = 3 \times 10^7$ cm/s and $v_A = 1 \times 10^8$ cm/s (LaRosa et al. 1996), this gives $\lambda_{SF}/L_T \sim 10^{-6}$. We have taken the initial electron velocity to be the mean velocity of the thermal background plasma. The cascade will proceed down the inertial range to this length scale where STFA then acts as the micro-physical damping agent, rapidly draining the energy from turbulence into particles.

In the case of the fast mode, where $v_c = v_A$, the rate balance is

$$\frac{2nm_e}{L_T} v_A^2 v \left(\frac{\lambda_T}{L_T} \right)^{(1/a)-1} = \frac{nm_p}{L_T} v_A^3, \quad (24)$$

and the STFA length scale is then given by

$$\frac{\lambda_{SF}}{L_T} = \left[\frac{1}{2} \frac{m_p}{m_e} \frac{v_A}{v} \right]^{\frac{a}{1-a}}. \quad (25)$$

For solar flare conditions, and a GS cascade ($a = 2$), $\lambda_{SF}/L_T = 10^{-4}$. We have tacitly assumed that the length scale for pitch angle isotropization is roughly equal to λ_T . If it is

not, the acceleration rate is retarded significantly, and STFA can be shut off. To understand this we must further explore the role of pitch angle scattering.

As discussed above, pitch angle scattering is necessary during acceleration to maintain a population of electrons which satisfy the pitch angle condition for reflection. The strength of the pitch angle scattering strongly regulates the rate of acceleration. We consider three cases: $\lambda_p \gg \lambda_{SF}$, $\lambda_p \ll \lambda_{SF}$, and $\lambda_p \sim \lambda_{SF}$ where eddy λ_p is the typical distance over which pitch angles are isotropized. In the first case, $\lambda_p \gg \lambda_{SF}$, electrons reflect a few times and quickly leave the pitch angle range in which they can reflect. They then must stream a distance of order λ_p before they can scatter again. Thus the rate of reflections and the acceleration rate are both decreased by a factor of λ_{SF}/λ_p . Since the acceleration rate and cascade rate are not in balance, the cascade continues down to smaller scales $\lambda_T < \lambda_{SF}$. The nominal acceleration rate (eq 22) is proportional to $\lambda_T^{-1/2}$, while the retardation factor is proportional to λ_T . The combined effect is a net acceleration rate which is proportional to $\lambda_T^{1/2}$; smaller scale turbulence is actually less efficient as an accelerator. As a result, STFA never turns on in this regime. In the second case, $\lambda_p \ll \lambda_{SF}$, the pitch angle scattering is far more rapid than acceleration. Since pitch scattering can take an electron through $\mu = 0$, very strongly pitch scattered electrons traverse the plasma by random walking in steps of length λ_p , again reducing the rate of reflection, this time by a factor of $(\lambda_p/\lambda_{SF})^2$. Unlike the previous case, this is not a problem for STFA; the retarding factor tends towards unity as the cascade continues to scales $\lambda_T < \lambda_{SF}$. The net acceleration rate is proportional to $\lambda_T^{-5/2}$, and STFA turns on as the cascade proceeds to a sufficiently small scale. In case three, where $\lambda_p \sim \lambda_S$, pitch angle scattering and reflections proceed at the same rate. Thus, electrons are capable of streaming freely from compression to compression, while they maintain a nearly isotropic pitch angle distribution. This is the simplest pitch angle scattering regime for STFA.

The identity of the accelerating wavemode is now easy to determine. In section 4.1 we show that whistler wave turbulence is a plausible source of pitch angle scattering, at least for the lower energy quasi-thermal component of the spectrum. At 3keV, λ_{wh}/L_T is roughly 10^{-4} . This places slow mode turbulence ($\lambda_{SF}/L_T \sim 10^{-6}$) well in the first regime. Slow modes do not participate in STFA in these flares. Fast modes, however, have $\lambda_{SF}/L_T \sim 10^{-4}$ and therefore are in the nearly ideal range for acceleration. Furthermore, both λ_{SF} and λ_p grow linearly with electron energy, so as electrons undergo STFA by fast modes in the presence of whistler wave turbulence, they remain in the same pitch angle scattering regime throughout.

4. The post-acceleration spectrum

The simplest case of STFA is the steady state, where we assume that electrons are injected into a turbulent region at energy E_0 at a rate equal to that at which accelerated electrons escape. The turbulent energy supply is continuously replenished at a large scale. We are concerned with the energy spectrum, $N(E)$, of electrons escaping the region. Note that this is in general different from the spectrum of the electrons within the turbulent region. We define $N_t(E)$ to be the total number of electrons reaching energy at least E before escaping, such that

$$N(E) \propto -dN_t(E)/dE. \quad (26)$$

Initially, we consider the case of strongly relativistic electrons; a full derivation of this regime is presented in the Appendix.

To appreciate the calculational differences between the non-relativistic regime of interest to solar flares and the more commonly studied relativistic regime, we begin with the latter. Following the approach used by Bell (1978) for Shock Fermi acceleration, and writing $dN_t/dM = -p_{esc}N_t$, where p_{esc} is the mean probability of an electron escaping from the acceleration region, gives

$$\frac{dN_t}{dE} = -\frac{dN_t}{dM} \frac{dM}{dE} = -p_{esc}N_t \frac{dM}{dE} = -p_{esc}N_t \frac{1}{\alpha E}, \quad (27)$$

where on the right hand side we have for the moment taken the strongly relativistic limit: $dE/dM = \alpha E$ and assumed p_{esc} to be constant. This treatment of the highly relativistic limit follows Fermi (1949). One can solve for $N_t(E)$ by separating variables, integrating both sides and inverting the logarithms, resulting in the familiar power law (see e.g. Fermi (1949); Longair (1994); Jones (1994))

$$N_t(E) = N \left(\frac{E}{E_0} \right)^{-\frac{p_{esc}}{\alpha}}, \quad (28)$$

where N is the total number of electrons. From Eq. (26), one obtains

$$N(E) = N_0 \left(\frac{E}{E_0} \right)^{-(1+\frac{p_{esc}}{\alpha})}, \quad (29)$$

where $N_0 dE$ is the number density of escaped electrons with $E = E_0$. Notice that the logarithmic integrals in both N_t and E are vital to producing the power law.

For STFA by fast mode waves, the computation is more complicated because p_{esc} is energy dependent. We solve for a general p_{esc} in the non-relativistic regime, leaving the

specification of the trapping for later discussion. In the non-relativistic regime, the acceleration rate is not proportional to the kinetic energy as it is in the strongly relativistic regime. Instead, one has $dE/dM = 4mv_A^2$. We thus write, using (11),

$$\frac{dN_t}{dE} = -\frac{N_t p_{esc}}{4mv_A^2}, \quad (30)$$

which can be rewritten as

$$\frac{dN_t}{N_t} = \frac{p_{esc}}{4mv_A^2} dE. \quad (31)$$

We have assumed that $dN_T/dM = p_{esc}N_t$. This is reasonable as long as the electrons can be treated as statistically independent and collisionless. In this case, it is reasonable to assume that p_{esc} carries no inherent dependence on N_t and the escape rate is simply given by the product of the number of electrons in the volume and the mean escape probability. Taking $p_{esc} = p_0(E/E_0)^{-1}$ allows us to solve for a particularly interesting $N(E)$. We see immediately that

$$\frac{dN_t}{N_t} = -\frac{E_0}{E} \frac{p_0}{4mv_A^2} dE, \quad (32)$$

and $N(E)$ is again a power law energy distribution:

$$N(E) = N_0 \left(\frac{E}{E_0} \right)^{-(1+\delta)}, \quad (33)$$

where $\delta = p_0 E_0 / 4mv_A^2$. However, in any other case, STFA does not produce a simple power law. The importance of the trapping mechanism is now clear; the combined energy dependence of the acceleration and escape must be E^{-1} to produce a power law spectrum. Such a spectrum relies on the coincidental logarithmic integrals over both N and E .

4.1. Calculation of p_{esc}

Let us now calculate p_{esc} for non-relativistic electrons within the turbulent volume, and consequently the energy spectrum of electrons. For simplicity, let us take the turbulent region to be rectangular, with the long axis, z , parallel to the direction of the bulk flow, with $z = 0$ and $z = L_F$ fixed to the downstream and upstream boundaries of the region respectively. L_F is taken to be the extent of the region of turbulent flow, which is presumed to be the entire distance between the reconnection sheet and the top of the soft X-ray loop.

This distance is typically of size 10^{10} cm for solar flares (Tsuneta 1996). The largest eddy size in the turbulence, L_T is set by the width of the outflow, typically 10^8 cm. Thus the turbulent volume consists of a number of cells, each of which flows downward from the reconnection point towards the loop-top. An electron escapes the acceleration region only when it reaches the X-ray loop at the base of the turbulent region. These individual cells may be associated with single bursts or fragments of X-ray emission, and thus are responsible for the temporal structure of impulsive flares. In order to escape the region with energy $E(M)$, an electron must stream from its location in the region at some height z to the boundary at $z = 0$ after the M th reflection without further reflection. We will assume that the electrons are contained in the region in the $x-y$ plane by gyration around large scale field lines. To further simplify the problem, we shall assume that the electron density remains uniform throughout the turbulent region. We also neglect the bulk flow speed, $v_f = 8 \times 10^7$ cm s $^{-1}$ (Tsuneta 1996) since the length of the downflow region is roughly 10^{10} cm. This gives a flow time from the reconnection region to the loop-top of 100s. The acceleration process is fixed to the much shorter 1s time scale by the temporal size of the observed energy release fragments and the MHD eddy turnover time. Thus, bulk flow into the flare loop is not likely to be a dominant process in cutting off the acceleration.

Take the mean z -component of the distance streamed between reflections to be λ_z ; λ_z carries an energy dependence inherited from the energy dependence of the pitch scattering. The probability of escaping at $z = 0$ after the M th reflection from a point at height z is given by

$$p_{esc}(z) = \frac{1}{2}e^{-z/\lambda_z}, \quad (34)$$

and the mean escape probability of electrons distributed uniformly across the length of the region is

$$p_{esc} = \frac{1}{L_F} \int_0^{L_F} p_{esc}(z) dz = \frac{\lambda_p}{L_F} (1 - e^{-2L_F/\lambda_p}), \quad (35)$$

where we have taken $\lambda_z = \lambda_p/2$ from the isotropy in pitch angles, with λ_p the pitch angle scattering length scale. To obtain the spectrum of solar flare electrons requires specification of the pitch angle scattering.

Both Miller, Larosa, & Moore (1996) and LaRosa et al. (1996) assume strong scattering, and suggest that the scattering agent above 1keV is resonant interaction with lower hybrid (LH) turbulence, or circularly polarized electromagnetic waves, such as whistler waves. Below 1keV, Coulomb interactions are thought to be sufficiently strong to isotropize the electrons. It should be noted that Melrose (1974) sets the threshold for the whistler mode resonance

at 25 keV for flare plasmas, while Miller & Steinacker (1992) argue that the resonances extend down to 1keV. We assume the latter. In a recent study, Luo, et.al. (2003) considered whether LH wave turbulence is the primary mode of electron acceleration in solar flares. They concluded that the pitch angle scattering is too inefficient to maintain isotropy. Thus, we assume that LH wave turbulence cannot supply sufficient pitch angle scattering to sustain STFA either. Whistler waves are more promising.

Melrose (1974) associates the frequency of pitch angle scattering ν with the pitch angle diffusion coefficient in the quasi-linear equation. Thus, $1/\nu$ is the characteristic time scale for effective pitch angle isotropization of the electron distribution. It should be noted that, in general, some small anisotropy is likely to remain in the distribution, and that this anisotropy could be responsible for the generation of the whistler waves. However, the source of these waves is still uncertain. From Melrose (1974), we have that

$$\nu = \frac{\omega_p^2 \epsilon(\omega_R)}{\gamma_e \Omega_e n_e m c^2}, \quad (36)$$

where $\gamma_e \sim 1$ is the Lorentz factor of the electron, Ω_e is the electron gyrofrequency, ω_p is the plasma oscillation frequency, and

$$\epsilon(\omega_R) = \frac{m_p n_p v_A^2}{2} \frac{\delta B}{B}, \quad (37)$$

is the energy density of the turbulence at the resonant wavelength. This allows us to rewrite (36) as

$$\nu = 5 \times 10^7 B_{100} n_{10}^{-1/2} \left(\frac{\lambda_T}{L_T} \right)^{1/2}, \quad (38)$$

where we have used $v_A^2 = B^2/4\pi n_p$, $\Omega_e = 1.8 \times 10^9 B_{100}$, $\omega_p = 5.7 \times 10^9 n_{10}^{1/2}$, and the dimensionless parameters $B_{100} = B/100\text{G}$ and $n_{10} = n_e/10^{10}\text{cm}^{-3}$.

We must compare ν to the growth time for pitch angle anisotropy due to STFA. Bearing in mind that for STFA, $dv_{\perp}/dt = 0$,

$$\frac{dE}{dt} = m v_{\parallel} \frac{dv_{\parallel}}{dt}, \quad (39)$$

and the pitch angle evolves according to

$$\frac{d(\cos \theta)}{dt} = \frac{1}{m v^2 \cos \theta} \frac{dE}{dt}. \quad (40)$$

Substituting in from equation (21) for dE/dt and assuming a GS cascade ($a = 2$), gives

$$\nu_{SF} = \frac{d(\cos \theta)}{dt} = \frac{2}{L_T} \left(\frac{\lambda_T}{L_T} \right)^{(-1/2)} \frac{v_A^2}{v} \frac{1}{\cos \theta}. \quad (41)$$

For impulsive flares, $E_0 = 0.3keV$, $B_{100} = 2$, and $n_{10} = 1$. Taking $\lambda_T = \lambda_{SF}$ results in $\nu = 1 \times 10^6 \text{ s}^{-1}$ and

$$\nu_{SF} = 2 \times 10^2 \left(\frac{E_0}{E} \right)^{1/2} \text{ s}^{-1}, \quad (42)$$

where ν_{SF} is evaluated at the threshold pitch angle for reflection. To maintain pitch angle isotropy, scattering by whistler waves must occur on a time scale shorter than pitch angle evolution by STFA. Thus, as long as $\nu_{SF} < \nu$, isotropy can be maintained. This condition is met for all $E > E_0$. Whistler modes, if present, are capable of providing sufficient pitch angle scattering to maintain isotropy.

In addition to maintaining pitch angle isotropy, the scattering mechanism must also operate at a length scale which traps electrons in the volume; $\lambda_{wh} \ll L_T = 10^8 \text{ cm}$ must be satisfied, or else electrons rapidly leave the acceleration region and STFA shuts off. We obtain the pitch scattering length scale for whistler waves, λ_{wh} ,

$$\lambda_{wh} = \frac{v}{\nu} = 2 \times 10^3 \left(\frac{E}{E_0} \right)^{1/2} \text{ cm}. \quad (43)$$

The required condition is satisfied for energies below 100keV.

4.2. The Electron Spectrum and Constraints on the Secondary Pitch Angle Scattering

In order to obtain the spectrum of the escaped electrons, we can now substitute the functional form for p_{esc} from (35) into (31)

$$\frac{dN_t}{N_t} = \frac{p_{esc}}{4mv_A^2} dE = \frac{\lambda_p}{L_F} (1 - e^{-L_F/\lambda_p}) \frac{1}{4mv_A^2} dE. \quad (44)$$

Next, by choosing $\lambda_p = \lambda_{wh}$, we use $\lambda_p/L_F = AE^{1/2}$, with E in units of keV, and rearranging, obtain

$$N(E) = \frac{dN_t}{dE} = AE^{1/2}(1 - e^{-1/AE^{1/2}})\frac{1}{4mv_A^2}N_t. \quad (45)$$

The resulting spectrum, $N(E)$, is plotted in figure 4. This is consistent with the thermal component to the flare spectrum observed using RHESSI (Krucker, & Lin 2002).

In addition to the thermal component, RHESSI observations show a clear power law region extending from roughly 10keV up to at least 50keV, above which the data are uncertain, but consistent with a continuing power law. Previous observations using the ISEE3/ICE instrument also show a power law throughout the range of the instrument, 25 – 300keV; the spectrum typically breaks downward at 100keV (Dulk et.al. 1992). More recent observations with RHESSI could push the low energy threshold for the power law as high as 35keV (Holman et. al. 2003). The spectral index below the break is ~ 3 , while above the break it is ~ 4 . Elsewhere (Blackman (1997); Selkowitz and Blackman (2004) in preparation), we discuss first order acceleration at the loop-top fast shock. Fast shocks are well known to accelerate super-thermal particles to power law energy spectra, even in the non-relativistic limit (Bell 1978). However, in order to be accelerated, electrons must satisfy the requirement that $E \gg (m_p/m_e)v_s^2 = 10\text{keV}$ in solar flare plasmas, where $v_s = 10^8\text{cm s}^{-1}$ is the inflow speed of the plasma at the shock (Blackman & Field 1994). This places the injection energy at roughly 100keV. The correspondence of the shock injection energy and the observed break energy is noteworthy. A possible mechanism to reproduce the observations is for STFA to produce a power law spectrum in the 10 – 100keV regime which then satisfies the injection criterion for loop-top fast shocks. Since STFA by magnetosonic turbulence in the presence of whistler wave turbulence pitch scattering is insufficient to produce the power law component. However, it is possible that a second pitch scattering agent exists which produces the power law in the 10 – 100keV range. We examine the constraints imposed on this scattering.

To produce a power law spectrum, non-relativistic STFA requires $p_{esc} \propto E^{-1}$. From (35), we see that this is true only if $\lambda_p/L_F = \Gamma/E$, where $2E/\Gamma \gg 1$ and the exponential term is small. Here Γ is a constant parameter which fixes the strength of the pitch scattering. While the physics of the pitch angle scattering is not well understood, this constrains the scattering mechanisms available to STFA. We define $\lambda_C = L_T\Gamma/E = 2 \times 10^7(E_0/E)\text{cm}$ to be the pitch scattering length scale of the constrained mechanism, and the electron spectrum is given by

$$N(E) = N_0 \left(\frac{E}{E_0} \right)^{-(1+\Gamma/(4mv_A^2))}. \quad (46)$$

Γ is constrained by the observed X-ray spectral index of $\gamma = 3$. It is a standard prediction of flare models (Brown 1971; Stepanov and Tsap 2002; Kiplinger, et.al. 1984) that the spectrum

of electrons accelerated above the loop-top is steeper than the spectrum of the thick target Bremsstrahlung X-rays emitted at the footpoints in solar flares. We assume that to match the RHESSI X-ray data requires an index ~ 4 for the electrons, or

$$\Gamma = 12mv_A^2 = 0.072keV = 0.17E_0. \quad (47)$$

The exponential term in p_{esc} is indeed small as $2E/\Gamma = 270$ at $E = 10keV$. The electron spectral index could conceivably be as high as 6, in which case $\Gamma = 0.28E_0$, and the exponential can still be safely neglected.

It is insufficient to merely produce the proper power law. The scattering agent must also be able to reproduce the transition from thermal to power law spectrum at the correct energy, E_c . We recall λ_{wh} to be the length scale of pitch angle scattering associated with whistler wave turbulence. In impulsive flares, $\lambda_p = \lambda_{wh}$ below E_c . Above E_c , $\lambda_p = \lambda_C$. To obtain E_c one sets $\lambda_{wh} = \lambda_C$. $E_c = 23keV$, which is consistent with the observed threshold of $\sim 10keV$.

There is one more important constraint imposed by the observations: the knee at 100keV. Dulk et.al. (1992) demonstrate a distinct downward break in the power law spectrum at roughly $E_{br} = 100keV$. The break energy varies somewhat from flare to flare, but is consistently observed in all of the impulsive flares in their sample. Unlike downward breaks, upward breaks are easily explained by the meshing of two acceleration mechanisms, as the shallow component which dominates above the break emerges naturally from beneath the steeper power law which dominates below. For upward breaks, E_{br} is the naturally occurring crossover point. The matching problem is much more difficult for knees in the absence of significant cooling on timescales of interest. Since the steep component is above the break energy and the shallow component below it, both must be truncated at the break energy. If either one extended beyond the break, then that one would overrun the other, and there would be no break at all. The most natural solution for a knee is a single acceleration mechanism which undergoes some transition at the break energy. One such example is the knee found by Bell (1978b) in the spectra of shock accelerated electrons at roughly 1GeV. This knee results from the transition from the non-relativistic to the relativistic regime. There is no apparent natural transition for STFA of electrons at 100keV. However, there is a well defined low energy cutoff for a power law spectrum at 100keV, the shock injection energy. The shock injection threshold is not only at the right energy, but is also a variable cutoff, depending on the ion temperature and local magnetic field strength, consistent with the variability in the observed E_{br} .

Bell (1978b) has shown that shock acceleration does not change the spectrum of electrons if the pre-shock spectrum is shallower than the post-shock spectrum which obtains from a

steep pre-shock spectrum. Shock Fermi acceleration cannot steepen a power law spectrum; it can only make it shallower. This is another difficulty for knee matching. The STFA spectrum must have a sharp cutoff at E_{br} in order to match the knee. This may not be an impossible condition to meet, especially as E_{br} may be greater than the injection energy, not precisely equal to it.

One natural cutoff occurs when $\lambda_C = \lambda_r$; acceleration will shut off when the cascade reaches the resistive scale. For slow modes in impulsive flares, $\lambda_r = 10^3 \text{cm}$ (LaRosa et al. 1996; Chandran 2003; Lithwick and Goldreich 2001), which for $\Gamma = 0.073 \text{keV}$ gives a cutoff energy of $7 \times 10^5 \text{keV}$, which is both too high and far outside of the non-relativistic regime. A possible solution is that the constrained pitch scattering has a maximum resonant threshold at E_{br} . Another possible solution is that yet another very strong pitch scattering mechanism has a threshold energy of E_{br} and a length scale $< \lambda_r$. Both of these solutions are presently ad hoc. This underscores the need for a more thorough understanding of pitch angle scattering in astrophysical plasmas. It also illustrates the limitations of STFA as an acceleration mechanism in solar flares; if STFA alone were to account for the spectrum from 10 – 100 keV, the tight constraints on the pitch angle scattering mechanism that we have identified are required.

5. Summary and Discussion

STFA in the non-relativistic limit behaves differently from highly relativistic STFA. At the core of these differences is the energy dependence of the electron velocity at low energies. Thus, unlike the relativistic case, both the rate of reflections and the probability of escaping the acceleration region at an energy E vary. Using a test particle approach, we have examined this behavior and derived the spectrum of post-acceleration electrons in a plasma under impulsive solar flare conditions.

For traditional STFA, where there is a minimum pitch angle constraint which determines whether an individual encounter results in reflection, it is seen that the steady acceleration rate can dominate over the diffusive acceleration rate. This arises from the averaging over pitch angles to evaluate $\langle \Delta E \rangle$. Some previous treatments of the generalized Fermi acceleration problem do not have such reflection conditions, and thus do not retain factors of the turbulent field strength, $\delta B/B$, when averaging. In those treatments, such as Longair (1994); Skilling (1975); Webb (1983), the steady and diffusive terms typically are seen to be of the same order. For some processes this is appropriate, however non-resonant STFA is not one of them. Thus, the phase space conditions for scattering by the acceleration mechanism can play a very significant role, even in cases where pitch angle isotropy is maintained.

The nature of the pitch angle scattering turns out to be the dominant factor in determining electron escape, and therefore the shape of the spectrum. We find that whistler wave turbulence, which is well studied in solar flares (Melrose 1974; Miller & Steinacker 1992), is an excellent source of pitch angle scattering which allows STFA to produce a quasi-thermal electron distribution that peaks at $E \approx 5\text{keV}$. This matches the lowest energy portion of the observed X-ray emission very well. However, to produce the power law spectrum observed in the range $\sim 10 - 100\text{keV}$ by STFA requires at least a second scattering mechanism. Matching the spectral index and the transition energy from quasi-thermal to power law spectrum requires an undetermined scattering mechanism which satisfies $\lambda_C/L_F = \Gamma/E$ with $\Gamma = 0.073\text{keV}$, and naturally becomes the dominant pitch angle scatterer at roughly 20keV .

If the constrained pitch angle scattering mechanism is discovered, it implies that the acceleration of electrons in solar flares is at least a two stage process. The first stage, STFA in the downflow region, produces both the quasi-thermal spectrum below $\sim 10\text{keV}$ and the lower half of the power law spectrum up to 100keV . To produce the highest energy electrons, as well as the spectral break at $E = 100\text{keV}$ requires a second acceleration mechanism at the top of the soft X-ray loop. We are further exploring the possibility that first order acceleration at a weak fast shock, formed as the downflow impacts the top of the closed flare loop, is responsible for electron acceleration to the highest observed energies. Acceleration at fast shocks is known to have an injection energy of roughly 100keV , and varies with temperature. This coincides with the break in the power law spectrum at 100keV , and is consistent with the variability observed by Dulk et.al. (1992) in E_{br} .

Recently, Chandran (2003) concluded, using quasi-linear theory, that STFA for slow modes is not viable in the $10\text{-}100\text{keV}$ regime. While we also find slow modes to be ineffective, differences between our paper and Chandran (2003) must be kept in mind. Chandran (2003) assumed that $dp/dt \propto p$ for STFA. While this is true in the strongly relativistic limit for STFA, we do not assume that this is true in the lower energy regime (see eq. 22). Second, unlike Chandran (2003) we do not assume herein that P_{esc} has to be energy independent. These two assumptions play a significant role in shaping electron spectra.

Another concern which can be raised about the effectiveness of STFA as the electron acceleration engine in impulsive flares is the total energetics of the process. Since STFA, as developed above, only is efficient in a short length scale regime where one also has $\delta B/B \ll 1$ it might seem that only a small fraction of the released flare energy is available for electron acceleration. This is not the case. The total energy contained in single turbulent cell is given by $(1/2)m_p v_A^2 n L^3 \sim 10^{26}\text{erg}$, where $n = 10^{10}\text{cm}^{-3}$ is the electron number density in the flare plasma. The energy in a single turbulent cell is similar to the energy contained in one X-ray

emission fragment. Although only a fraction of the energy in one turbulent cell is ever at λ_p at one time, it does all cascade down to λ_p over an eddy turnover time. Thus, while $\delta B/B$ is always small, the energy throughput can still be high enough to accelerate the electrons. The similarity in total energy between a single turbulent cell and an individual impulsive X-ray fragment strongly suggests that the two are related.

Miller, et.al. (1997) estimates that as much as $\simeq 94\%$ of the magnetic energy in a flare is available in the turbulence, which is sufficient to produce the high energy electrons inferred from the observed X-rays, but raises concerns about the efficiency of STFA, particularly in competition with other sources of dissipation. While we have not fully studied other dissipation mechanisms which might compete with STFA for this energy, three significant ones can be ruled out: proton acceleration by STFA, Landau damping, and resistive dissipation of the turbulence. The latter two have already been discussed. Proton acceleration is a significant concern since Fermi acceleration of protons and heavy ions was in fact the very problem Fermi intended to solve. Thermal protons in coronal flare plasmas are sub-Alfvénic and thus cannot meet the condition for mirroring (LaRosa et al. 1996; Blackman 1999). However, Miller and Roberts (1995) argues convincingly that gyroresonant interaction of protons and heavy ions with Alfvén waves can accelerate them to velocities above v_A on a relatively short time scale. Within their model, the ions then are accelerated by compressive magnetosonic waves at the expense of electron acceleration. Recent RHESSI observations (Hurford et.al. 2003) indicate that the emission signatures of ions and electrons are spatially separated, with the ion emission associated with longer loops. Miller, Emslie, and Brown (2004) concluded that these observations are consistent with the gyroresonance model of ion acceleration; as the loops grow longer, protons are more likely to reach super-Alfvénic speeds, and thus can be accelerated by the magnetosonic waves. This second phase of acceleration need not be gyroresonant. While it appears promising, further study is required to determine if STFA models can accommodate these results.

The strong dependence of the post-acceleration electron spectrum on the pitch angle scattering agent is both a positive and negative feature. It leaves STFA considerable flexibility in matching various characteristics of solar flare X-rays which fall outside of the simple scenario studied in this paper. For example, Lin et.al. (1981) first observed a superhot component in a solar flare, which has since been supported by RHESSI observations Krucker, et.al. (2003). This thermal, or nearly thermal, spectral component is seen at energies of up to 35keV. Within our STFA framework, the superhot emission can easily be explained by an enhancement of pitch angle scattering at lower energies, either by increased whistler wave turbulence, or some other scattering agent. While this flexibility naturally allows for the wide range of flare characteristics observed, it does not yet definitively solve the flare acceleration problem. Instead, it shifts the focus exclusively to a well constrained, but largely

unspecified, array of pitch angle scattering mechanisms. This is the single greatest obstacle to STFA models of acceleration.

In short, STFA can naturally account for the thermal spectrum below 10keV, and somewhat less naturally for the non-thermal spectrum between 10keV and 100keV. There we have shown that λ_p must depend inversely on particle energy, in contrast to that of pitch angle scattering by whistler waves below $\sim 10\text{keV}$, which is proportional to the particle energy. Above 100keV, shock acceleration is a natural possibility; the needed injection of super-thermal electrons may be provided by STFA operating at energies below E_{br} . The knee at 100keV remains the most difficult spectral feature to accommodate, and we have explained the difficult requirements to pitch angle scattering that this demands.

E.B. thanks B. Chandran for discussions. We thank J. Maron for sharing the results of his simulations and acknowledge support from DOE grant DE-FG02-00ER54600 and the Laboratory for Laser Energetics at the University of Rochester. RS acknowledges support from the DOE Horton Fellowship. We also acknowledge the insightful critique and comments of the reviewer.

Appendix A: The Power Law Spectrum of Relativistic STFA

Notice that the spectrum we obtain for STFA is different from the power law result of Jones (1994). This is a matter of regime; we discussed in the text the acceleration of non-relativistic particles in a region of non-relativistic turbulence, here we show that when the particles are relativistic, a power law spectrum emerges.

Recall that (5) for fully relativistic electrons in a region of non-relativistic turbulence is given by (6)

$$\delta E_{\pm R} = 2E \left[\pm \frac{v_A v_{\parallel}}{c^2} + \frac{v_A^2}{c^2} \right],$$

where E is the total energy, kinetic plus rest, of the electron before reflection. Notice that if we take the low velocity limit, $v \ll c$ where $E = mc^2$, the expression reduces to (5). The relative velocity between the compression and electron for head-on and catch-up type interactions are still given by (8) so the steady acceleration rate is given by

$$\left(\frac{dE}{dt} \right)_S = 2E \left[(R_+ - R_-) \frac{v_A v_{\parallel}}{c^2} + R \frac{v_A^2}{c^2} \right] = 4 \frac{F v_A^2}{\lambda c^2} v_{\parallel} E. \quad (48)$$

Alternatively, we can find the mean acceleration per reflection by multiplying equation 48 by R^{-1}

$$\left(\frac{dE}{dl}\right)_S = 4\frac{v_A^2}{c^2}E. \quad (49)$$

In the highly relativistic limit, E is just the kinetic energy, and we recover the familiar result (Jones 1994) that $dE/dt \propto E$. This proportionality is expected to produce a power law. We derive the power law spectrum for STFA of highly relativistic electrons by following the approach of Bell (1978) and assume that p_{esc} is a constant in flare plasmas, independent of electron energy. We start by integrating dE/dl to obtain $E(l)$

$$l = \frac{1}{A} \ln(E/E_0), \quad (50)$$

$$A = \frac{4v_A^2}{c^2}.$$

The probability of an electron remaining in the acceleration region for at least l reflections is given by

$$P(l+) = (1 - p_{esc})^l. \quad (51)$$

Taking the logarithm and substituting in for l from equation 51, gives

$$\ln P(E+) = l \ln(1 - p_{esc}) = \frac{1}{A} \ln\left(\frac{E}{E_0}\right) \ln(1 - p_{esc}) = \ln\left(\frac{E}{E_0}\right)^{(-p_{esc}/A)-1}. \quad (52)$$

where we used the approximation $\ln(1 - p_{esc}) = -p_{esc}$ for $p_{esc} \ll 1$ in obtaining the expression to the right of the final equals sign. Differentiating with respect to E , results in

$$P(E) = E_0 \left(\frac{E}{E_0}\right)^{(-p_{esc}/A)-1}, \quad (53)$$

where $P(E)dE$ is the unnormalized probability of a post-acceleration electron having the energy E . In the limit, where p_{esc} is extremely small, the relativistic STFA spectrum has power law index ~ 1 . In a plasma where $p_{esc} \sim A$, the power law index can grow larger, and the index is very sensitive to p_{esc} . In the third regime, where $p_{esc} \gg A$, electrons stream out of the turbulent volume quickly, do not experience much acceleration, and have a very steep power law energy distribution with virtually no very high energy electrons ($E \gg E_0$).

Appendix B: Derivation of Steady Acceleration Rate with $F_+ \neq F_-$

In section 3.1 we derived the steady acceleration rate for electrons in a low β turbulent magnetic plasma. This derivation was contingent on the assumption that $F_+ = F_- = F$, which is not strictly valid. Blackman (1999) calculates F for Fermi acceleration. By resetting the limits of the integral in his eq (12), and renormalizing for the smaller phase space, one arrives at

$$F_{\pm} = \cos \phi_m \left[\pm \frac{v_A}{v} + \left(1 - \left(\frac{v_A}{v} \right)^2 (1 - \cos^2 \phi_m) \right)^{1/2} \right], \quad (54)$$

where $\cos \phi_m$ is the minimum pitch angle at which an electron will reflect and v_A/v is the ratio of the Alfvén speed to the electron speed. We rename these quantities A and B respectively; both are small quantities. By taking a series expansion of eq (54) and truncating it at second order in B , it can be simplified to

$$F_{\pm} = A \left[1 \pm B - \frac{1}{2} B^2 \right]. \quad (55)$$

Recall that from (8),

$$R_{\pm} = F_{\pm} \left(\frac{v_{\parallel} \pm v_A}{2\lambda} \right) = A \left[1 \pm B - \frac{1}{2} B^2 \right] (A \pm B) \frac{v}{2\lambda}. \quad (56)$$

From this one easily obtains

$$R = (R_+ + R_-) = \frac{v}{\lambda} \left[A^2 \left(1 - \frac{1}{2} B^2 \right) + AB^2 \right], \quad (57)$$

and

$$(R_+ - R_-) = \frac{v}{\lambda} \left[A^2 B + AB \left(1 - \frac{1}{2} B^2 \right) \right]. \quad (58)$$

This gives us all of the ingredients for calculating the steady acceleration from (7)

$$\left(\frac{dE}{dt} \right)_S = 2m[(R_+ - R_-)v_{\parallel}v_A + (R_+ + R_-)v_A^2].$$

The resulting acceleration rate is

$$\left(\frac{dE}{dt}\right)_{sb} = \frac{2mv^3}{\lambda} AB^2 \left[2A + A^2 - \frac{1}{2}B - \frac{1}{2}AB^2 + B^2 \right], \quad (59)$$

where we have added the additional subscript b to indicate the distinction from the previously calculated rate. The steady acceleration rate found in (10) from the assumption $F_+ = F_- = F$ is

$$\left(\frac{dE}{dt}\right)_s = \frac{4mv^3}{\lambda} A^2 B^2. \quad (60)$$

Note that provided $A > 4B$ this is the largest term in (59). Indeed, for coronal flare plasma, $B \sim 0.1$ at electron energy E_0 and decreases with increasing energy while $A \sim 0.1$ as well at E_0 , but is largely insensitive to electron energy. At the onset of the power law regime, $E = 10keV = 30E_0$, and $B \sim 0.01$; all terms of order B^3 or higher can be neglected, as can the term in A^3 . Thus we can safely use the assumption $F_+ = F_- = F$ in this regime, and (11) is reasonable.

REFERENCES

- Achterberg A. 1981, A&A, 98, 161
- Achterberg A. 1984, Advances in Space Research, 4, 193
- Aschwanden M.J., Schwartz R.A., Alt D.M., 1995, ApJ, 447, 923
- Axford W. I., Leer E., Skadron G. 1978, International Cosmic Ray Conference, 15th, Plovdiv, Bulgaria, August 13-26, 1977, Conference Papers. Volume 11. (A79-44583 19-93) Sofia, B'lgarska Akademiia na Naukite, 1978, p. 132-137., 11, 132
- Blackman E.G., Field G.B., Phys. Rev. Lett., 73, 3097
- Blackman E.G., 1997, ApJ, 484, L79
- Blackman E.G., 1999, MNRAS302, 723
- Bell A.R., 1978, MNRAS, 182, 147
- Bell A.R., 1978, MNRAS, 182, 443
- Blandford, R. & Eichler D. 1987, Phys. Rep., 154, 1
- Brown J.C., 1971, Sol. Phys., 18, 489B

- Chandran B.D.G., 2003, ApJ, 599, 1426
- Dendy R.O., 1990, Plasma Dynamics. Oxford University Press, New York
- Dulk G.A., Kiplinger A.L., Winglee R.M., 1992, ApJ, 389, 756
- Fermi E. 1949, Physical Review, 75, 1169
- Fermi E., 1954, ApJ, 119, 1F
- Goldreich P., Sridhar S., 1997, ApJ, 485, 680
- Holman G.D., Sui L., Schwartz R.A., Emslie A.G., 2003, ApJ, 595, 97
- Hurford G. J., Schwartz R. A., Krucker S., Lin R. P., Smith D. H., Vilmer N. 2003, ApJ, 595, L77
- Jones F. C. 1994, ApJS, 90, 561
- Jones F. C. & Ellison D. C. 1991, Space Science Reviews, 58, 259
- Kiplinger, A.L., Dennis, B.R., Frost, K.J., Orwig, L.E. 1984, ApJ, 287, L105
- Krucker S., Hurford G.J., Lin R.P., 2003, ApJ, 595, L103
- Krucker S., Lin R.P., 2002 Sol. Phys., 210, 229
- Krymskii G. F. 1977, Akademiia Nauk SSSR Doklady, 234, 1306 (translation in Soviet Physics - Doklady, vol. 22, June 1977, p. 327,328.)
- LaRosa T.N., Moore R.J., Miller J.A., Shore S.N., 1996, ApJ, 467, 454
- Lin R.P., Schwartz R.A., Pelling R.M., Hurley K.C., 1981, ApJ, 251, L109
- Lithwick Y., Goldreich P., 2001, ApJ, 562, 279L
- Longair M. S., 1994, High Energy Astrophysics vol.2, Cambridge University Press, Cambridge
- Luo Q.Y., Wei F.S., Feng X.S., 2003, ApJ, 584, 497
- Masuda S., Kosugi T., Tsuneta S, Hara H., 1996, Adv. Space Res., 17, 63
- Melrose D.B., 1974, Sol. Phys., 37, 353
- Miller J.A., et.al., 1997, J. Geophys. Res., 102, 14631

- Miller J.A., Emslie A.G., Brown J.C., 2004, ApJ, 602, L69
- Miller J. A., Larosa T. N., Moore R. L. 1996, ApJ, 461, 445
- Miller J.A., Roberts D.A., 1995, ApJ, 452, 912
- Miller J.A., Steinacker J., 1992, ApJ, 399, 284
- Park B.T., Petrosian V., 1996, ApJ, 446, 699
- Park, B.T., Petrosian V., Schwartz R.A., 1997, ApJ, 489, 358
- Skilling J., 1975, MNRAS, 172, 557
- Spitzer L., 1956, Physics of Fully Ionized Gases. Interscience, New York
- Stepanov, A.V., Tsap, Y.T., 2002, Sol. Phys., 211, 135
- Tandberg-Hanssen E., Emslie A.G., 1988, The Physics of Solar Flares. Cambridge University Press, Cambridge
- Tsuneta S., 1996, ApJ, 456, 840
- Webb G.M., 1983, ApJ, 270, 319

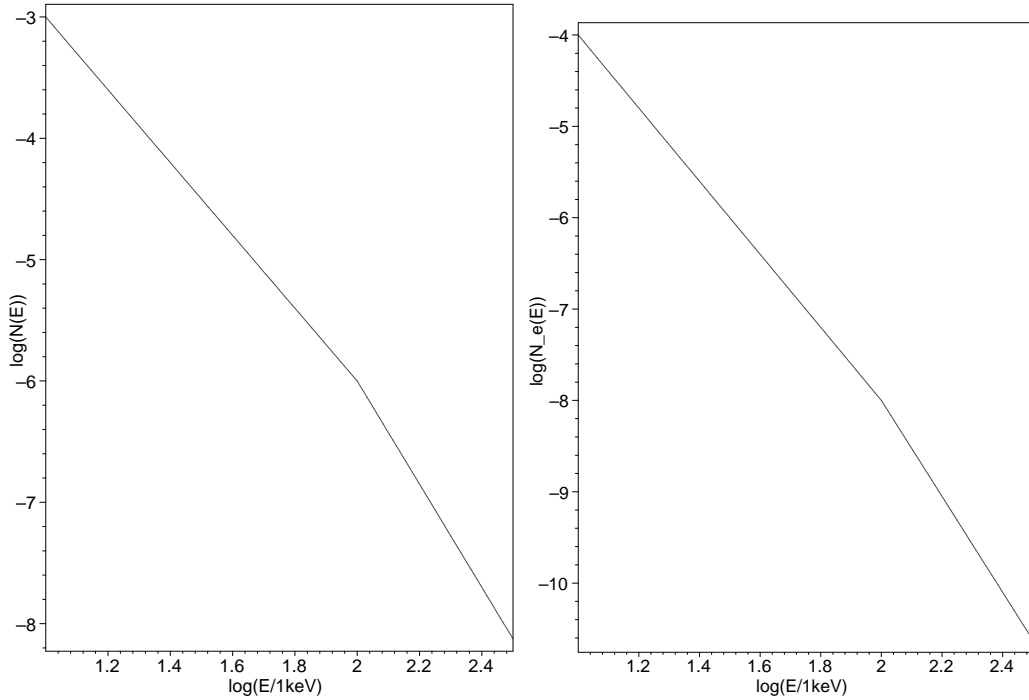


Fig. 1.— The typical downward broken power law of an impulsive flare, as observed by Dulk et.al. (1992). The left panel shows the hard X-ray spectrum, with $E_{br} = 100keV$, and spectral indices above and below E_{br} of 4.25 and 3 respectively. The right hand panel shows the electron spectrum in the emission region inferred from the given photon spectrum using a thick target Bremstrahlung model for the emission (Brown 1971; Tandberg-Hanssen & Emslie 1988). Again, $E_{br} = 100keV$ and the spectral indices above and below E_{br} are 4 and 5.25.

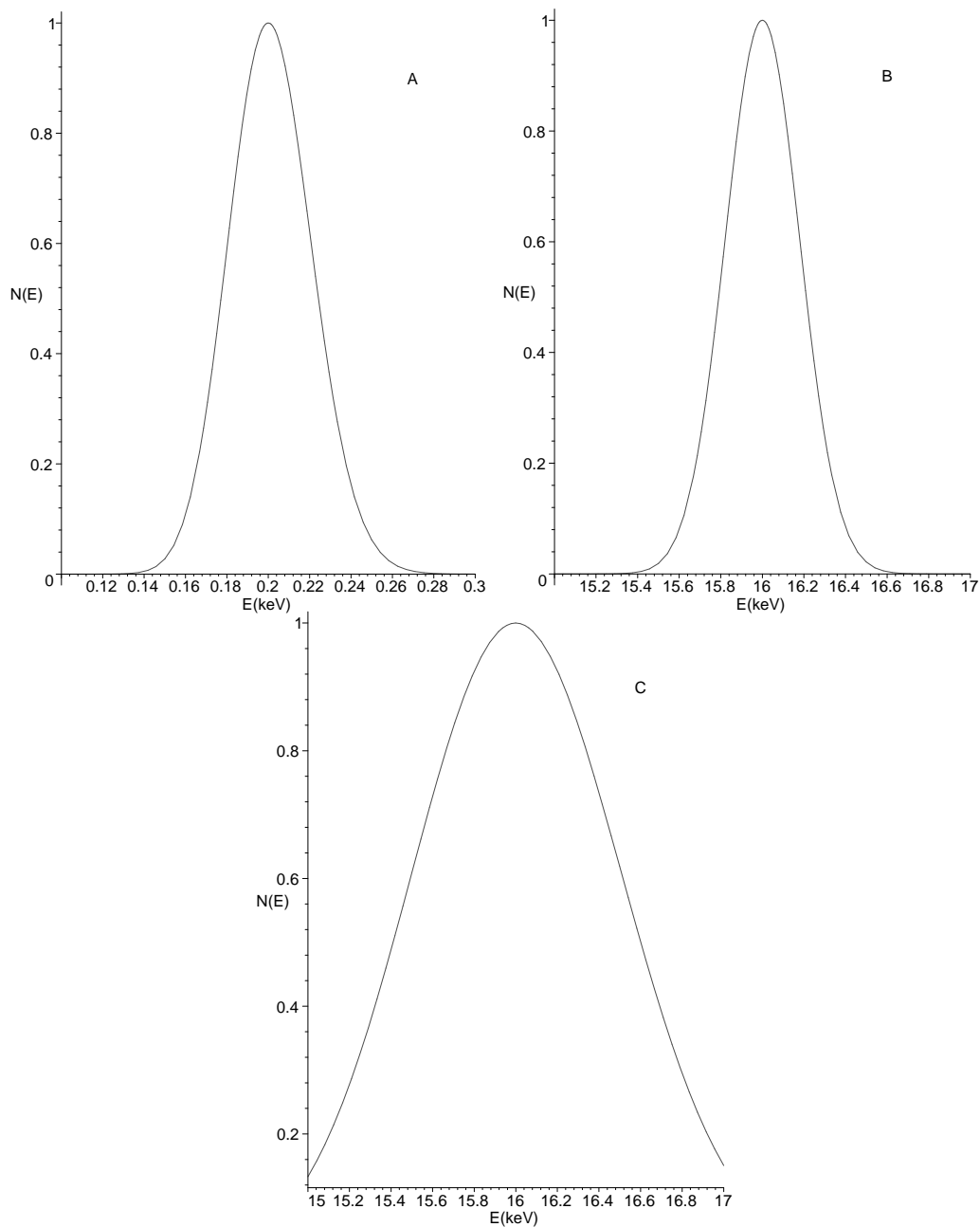


Fig. 2.— The evolution of a sample electron energy distribution with an initially Gaussian velocity distribution. The peak of the distribution is evolved from the flare thermal energy, 0.2keV to the post-STFA mean energy at 16keV. A) The initial distribution function. B) The same distribution after being evolved only by the steady process. C) The distribution evolved through both the steady and diffusive processes. Note that the relative width of the electron energy distribution, $\Delta E/E_m$ decreases with increasing mean energy E_m .

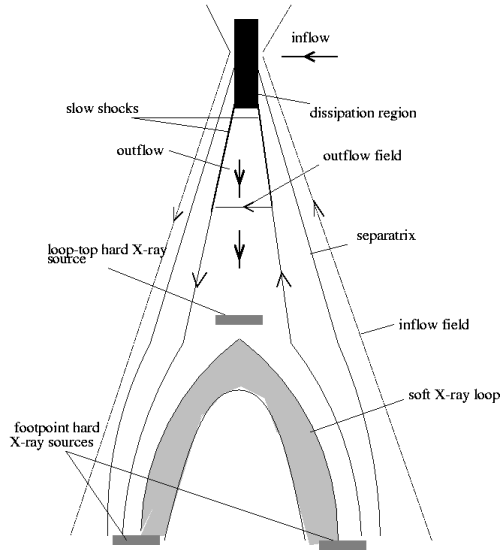


Fig. 3.— From (Blackman 1997). Sketch of a typical impulsive solar flare. Note that the x-point reconnection occurs in the filled region at the top of the diagram. Only the downward half of the outflow is shown. Reproduced by permission of the AAS.

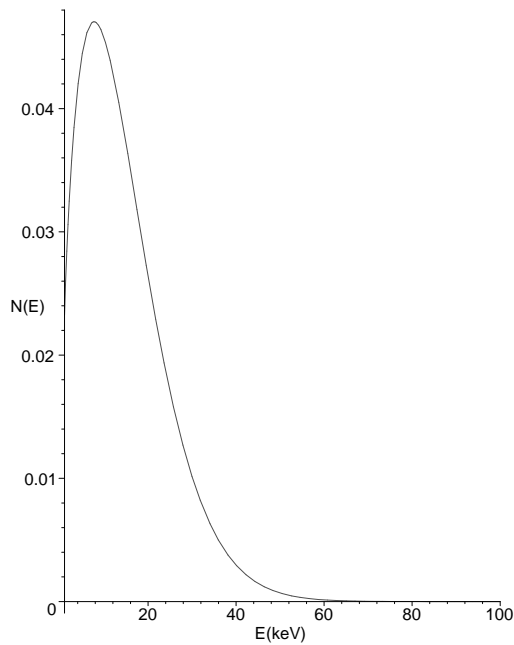


Fig. 4.— The spectrum of non-relativistic STFA under impulsive flare conditions with whistler wave turbulence as the only pitch angle scatterer. $E_0 = 0.3\text{keV}$.

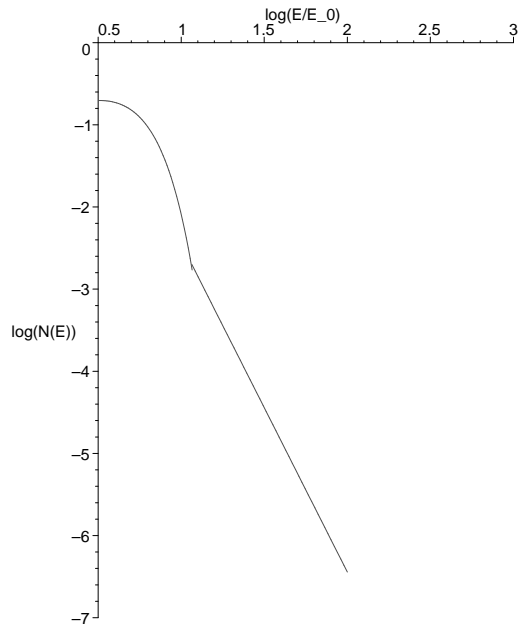


Fig. 5.— The spectrum of non-relativistic STFA under impulsive flare conditions with whistler wave turbulence and a second source of pitch angle scattering. The second pitch angle scattering source obeys the constraints required to produce a power law. $E_0 = 0.3\text{keV}$.